ELSEVIER

Diamond and Related Materials 9 (2000) 1222–1227

DIAMOND AND RELATED MATERIALS

www.elsevier.com/locate/diamond

Studies of phosphorus doped diamond-like carbon films

M-T. Kuo [a], P.W. May [a,*], A. Gunn [a], M.N.R. Ashfold [a], R.K. Wild [b]

[a] *School of Chemistry, University of Bristol, Bristol BS8 1TS, UK*
[b] *Interface Analysis Centre, University of Bristol, St Michael's Hill, Bristol BS2 8BS, UK*

Abstract

Phosphorus doped diamond-like carbon (DLC) films have been deposited on Si substrates using CH_4-based RF plasmas with addition of 0–21% PH_3 into the source gas mixture. Scanning Auger studies reveal that the films contain P:C ratios as high as 0.89, and that the degree of P incorporation is roughly proportional to the PH_3 concentration in the gas phase. Reduction in intensity and finally loss of the laser Raman G-band with increasing P content in the film shows that excessive P incorporation causes amorphisation of the film. The electronic properties of the films, such as field emission threshold and optical band gap, are a complicated function of film composition. Minimum field emission thresholds occur at P:C ratios of around 0.02, and voltage bias values ~30% lower than that for the undoped film. Annealing in vacuum at 150°C can improve the field emission threshold of the low P content films by a factor of four. © 2000 Elsevier Science S.A. All rights reserved.

Keywords: Carbon phosphide; Diamond-like carbon; Field emission; Phosphorus doping

1. Introduction

DLC films have been studied as a possible material for use in cold cathode devices and field emission displays (FEDs) because of their low surface work function, low temperature deposition and compatibility with existing microelectronic processing technology [1]. Doping of DLC films with nitrogen has been suggested as a method of improving their electronic properties [2] allowing control of film conductivity and optimisation of field emission. Most previous studies have concentrated on N as a dopant [3], and films with ≤40% N content have been reported [4]. N-doping has been variously reported to improve electrical performance giving field emission thresholds as low as $0.5\ \mathrm{V\ \mu m^{-1}}$ [5] but, conversely, some reports show that N-doping can degrade field emission performance [6]. A possible alternative dopant to nitrogen is phosphorus. Additions of PH_3 into the traditional CH_4/H_2 gas mixture [7] have been used to produce n-type chemical vapour deposited (CVD) diamond films [8] but, to date, there have been few reports of attempts to do the same with DLC films [9–13]. Veersamy et al. [10] incorporated up to 1% P into DLC (or tetrahedral amorphous carbon) films produced by a filtered cathodic arc method using a red phosphorus-doped carbon cathode, and found that P addition can reduce the resistivity of the films by 6–7 orders of magnitude, with no apparent change to the amorphous nature of the carbon films. Capacitively-coupled radio frequency (RF) plasma deposition has been used to produce P-doped DLC films [9,11] using PH_3 as a dopant gas giving films with P contents estimated to be ~11 at.%. These films, too, showed increases in room temperature conductivity of nearly five orders of magnitude, with resistivities which were strongly dependent upon the deposition temperature. Golzan et al. [12] showed that when films were doped with ~3% P, the dopant destabilised the tetrahedral network in favour of an sp^2 bonded network.

In this work, we have investigated the effect of a wide range of P content on the growth rate and electronic properties of DLC films. In particular, we present the results of the first field emission studies from P-doped DLC films and their variation with P content.

2. Experimental

Film deposition was carried out in a 13.56 MHz capacitively-coupled RF parallel plate plasma reactor. The gas feedstock was a mixture of CH_4 (maintained at

---

* Corresponding author. Tel.: +44-117-928-9927; fax: +44-117-925-1295.
E-mail address: paul.may@bris.ac.uk (P.W. May)

0925-9635/00/$ - see front matter © 2000 Elsevier Science S.A. All rights reserved.
PII: S0925-9635(99)00305-2

a constant flow of 30 sccm) and PH_3 (0 to 8 sccm) at a process pressure of 60 mTorr. 35–60 W of applied RF power was used to maintain a constant DC self-bias on the powered electrode of −150 V during deposition. The substrates were placed on this powered electrode. These substrates were 1 cm^2 mirror polished single crystal Si (100) — or quartz when investigating film transmission in the infrared and ultraviolet. The substrates were cleaned prior to deposition using isopropanol and then dried by N_2 gas. A deposition time of 30 min resulted in DLC films with various compositions and thicknesses (depending on the gas mixture); the latter were determined by cross-sectional scanning electron microscopy (SEM). Wavelength dispersed spectra of the plasma emission arising from the various process gas mixtures were recorded using an Oriel InstaSpec IV spectrometer over a range of 300–600 nm with a resolution of ~0.3 nm.

Sample composition was obtained using scanning Auger spectroscopy which provides a measure of the P:C content in the films but is insensitive to H. The Auger spectra were first differentiated to give a plot such as that shown in Fig. 1, and the peak-to-peak height for C and P were measured. These values were then corrected for sensitivity using the known elemental sensitivity factors for 10 keV incident electrons [14]. The major sources of error in this composition determination (estimated at ±10%) derive from changes in peak width with chemical bonding.

Film structure was examined by laser Raman spectroscopy operating at an Ar^+ laser wavelength of 514.5 nm. Fourier Transform infrared (FTIR) absorption spectroscopy was used to identify the characteristic bonding, and ultraviolet–visible absorption spectroscopy enabled determination of the optical band gap by the Tauc plot [15] — the usual method for amorphous materials. Field emission testing was performed in a high vacuum chamber (working pressure 10^{-7} Torr) which has been described in detail previously [6]. Briefly, the substrate was attached to a grounded electrode using electrically conducting glue. A hemispherical copper counter electrode of diameter 0.5 mm was positioned at a user selected distance a few tens of μm from the surface of the DLC film and was biased positively using a high voltage power supply. The bias voltage was ramped using a computer and the emission current measured using a picoammeter. Care was taken not to draw too much current which could result in obvious damage to the DLC film [16], and films were inspected by SEM after testing to ensure there was no surface damage. In this work, field emission thresholds are defined as the potential at which the emission current exceeds 10 nA (i.e. $>5\ \mu A\ cm^{-2}$ — a value consistent with operation of high brightness display applications).

It was found that the conductivity, and hence the field emission voltage, of the films changed markedly with time and exposure to air. This was especially true for films with high P content, and we believe that this is due to reactive P atoms within the film oxidising to form PO_x species on or near the surface. The presence of PO_x species in samples which have been exposed to air was confirmed by SIMS analysis. In order to obtain repeatable field emission results, therefore, the samples were transferred to the field emission chamber immediately upon removal from the deposition chamber and kept under high vacuum until the testing was performed.

After testing, some of the films were annealed in vacuum ($<10^{-5}$ Torr) for 30 min at 150°C in an attempt to drive off hydrogen and cause the C and P to react together to form a more ordered and structurally bonded compound. These films were then re-tested and their field emission properties compared to the as-grown samples.

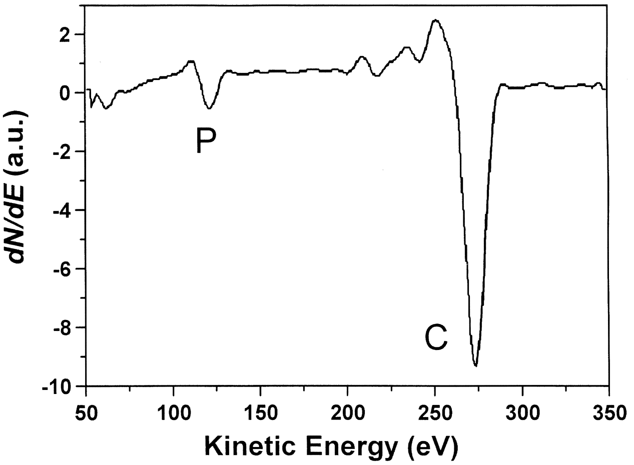

Fig. 1. Scanning Auger spectrum recorded for a film grown using 1.64% PH_3 in CH_4 at an incident electron energy of 10 keV, after differentiation, showing peaks characteristic of P and C.

3. Results and discussion

The P-doped DLC films were smooth on a nanometer scale, uniform in thickness and exhibited a variety of colours dependent on their thickness. Using a simple mechanical scratch test we found that, in general, the films with high P doping levels were softer than undoped films grown with pure CH_4. Films with P:C ratios <0.05 could not be scratched with metal tweezers, whereas those with P:C>0.05 could be scratched easily.

The compositions of various DLC films grown with different PH_3/CH_4 gas mixing ratios are shown in Fig. 2. Evidently, the amount of P incorporated into the film scales with the gas phase PH_3 content. For the highest PH_3 flow rate, the resulting film had a P:C ratio approaching 1. Such a film should probably be considered to be a form of 'amorphous carbon phosphide'

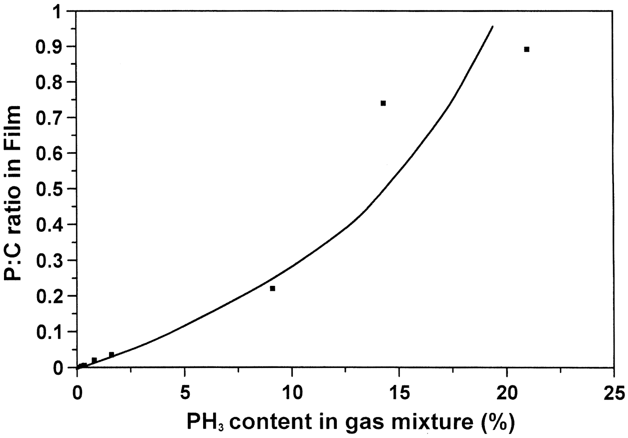

Fig. 2. Plot of the P:C ratio in the films (measured by scanning Auger spectroscopy) vs. PH_3 content in the process gas mixture. Errors in the P:C ratio are estimated at ±10% of the value and a line has been drawn connecting the points to guide the eye. The growth conditions are given in the main text.

rather than doped DLC. Unfortunately, Auger analysis cannot measure H content and so this remains an unknown, which is why throughout this paper we quote P:C ratios rather than elemental percentages within the film. However we can suggest an estimate for the approximate H content of these films, since we know from microcombustion experiments that the undoped films grown in the same apparatus have H contents of around 10%. Also, in our previous experiments with N-doped DLC films [6] we found that the H concentration remained roughly constant at around 8–11%, and was almost independent of the source of nitrogen (N_2 or NH_3) or the doping level. If we assume that this finding also holds true for the present PH_3 experiments, then for the film grown using 79% CH_4/21% PH_3 the true film composition would be ~10% H, 43% P, 47% C.

The plasma exhibits optical emission features in the wavelength range monitored which are attributable to CH (431 nm) and H_β (486 nm), the P containing species PH (339–343 nm) and PH^+ (368, 388 and 426 nm), and some peaks attributable to N_2 impurities in the chamber. The PH and PH^+ band intensities increase in proportion to increases in the gas phase PH_3 content, whilst the peaks of CH and H_β show constant intensities. This indicates that, once calibrated against film composition, the PH and PH^+ emission bands could be used for process monitoring and optimisation.

The film growth rate versus gas phase PH_3 content is shown in Fig. 3. Each point on the graph was repeated at least twice on separate days to check repeatability. It can be seen that the growth rate is not a smooth function of gas composition. Initially even very small (<0.2%) additions of PH_3 reduce the growth rate by ~30%. The reason for this is unknown. Thereafter, further additions of PH_3 improve the growth rate, with a maximum improvement of ~25% occurring at a PH_3 concentration of 1.25%. With still further PH_3 additions, the growth rate decreases again until a minimum is reached at 3%, then at still higher PH_3 flows the growth rate increases again. The reason for this complicated behaviour is not known, but it is likely to be the result of a combination of processes, including destabilisation of the plasma due to the presence of electronegative P-containing species, increasing incorporation of P species into the film and the gradual amorphisation of the film.

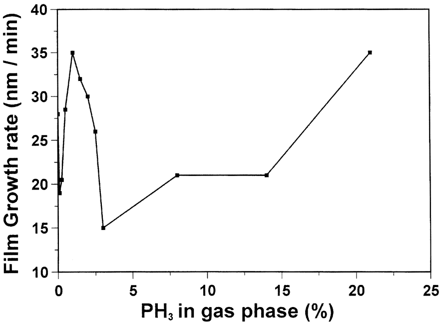

Fig. 3. Film growth rate plotted as a function of PH_3 addition into the gas phase. A line has been drawn connecting the points to guide the eye.

FTIR absorption spectra of films deposited with low PH_3 flow rates on quartz substrates show several maxima in the range 2850–2950 cm^{-1} characteristic of CH_x vibrations [17]. These CH_x absorption peaks decrease with increase in PH_3 flow rate, but no new features due to PH_x stretching modes (at ~2200–2400 cm^{-1}) were observed. Noticeably, in films with high P content (P:C>0.1), another feature gradually appears in the FTIR spectrum as a shoulder at ~2886 cm^{-1} becoming more apparent as the other CH_x peaks reduce in intensity. This feature could be sp^3 bonded CH which had previously been masked by the larger CH_x peaks, or arises from formation of further sp^3 bonded carbon, or is a chemical shift of one of the other peaks due to the formation of C—P chemical bonds. Evidence for the latter comes from SIMS analysis of the films which shows peaks at *m*/*e* values of 43, 55 and 67 attributed to C_xP ($x=1$–3) clusters, suggesting that some of the P is chemically bonded to C within the films. Other peaks at *m*/*e* values of 47, 63 and 79 showed the presence of PO_x ($x=1$–3) species on the surface of the films.

Fig. 4a shows laser Raman spectra taken from a number of films with different P content. For films grown with low P content, the graphite G-band is seen centred at ~1520 cm^{-1} along with a broad feature at ~1180 cm^{-1} often associated with nanocrystalline sp^3 carbon [18]. These two features decrease with increasing PH_3 flow rate until for P:C ratios >0.79 they have disappeared. Fig. 4b shows the position of the G-band centre and its FWHM plotted as a function of P:C ratio in the film. The G-band is associated with ordered graphite (or sp^2 carbon) and from Fig. 4b we see that at low P content the FWHM decreases slightly whilst

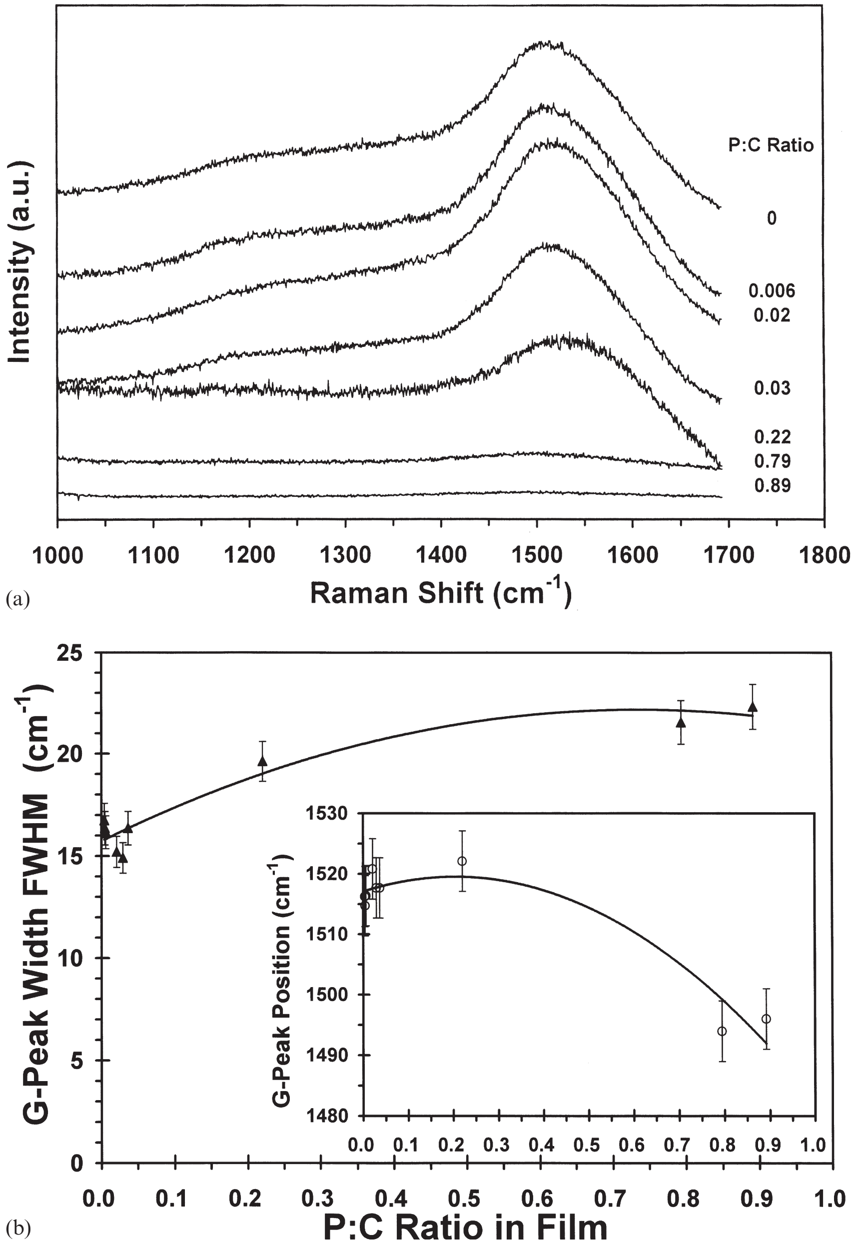

Fig. 4. (a) Laser Raman spectra of films grown with different P:C ratios in the film — the spectra have been plotted on a common vertical scale but offset vertically for clarity. (b) The FWHM of the laser Raman G-peak and the position of the peak centre (inset) plotted as a function of P:C ratio in the films.

its position increases closer to 1520 cm^{-1}, suggesting that these hard films are more ordered. At higher P contents the G-peak position decreases and its FWHM increases, with the G-peak eventually flattening out and disappearing, suggesting that at these high P contents the structure is being amorphised. Thus, the structure of the films with higher P content can be envisaged as an amorphous matrix of randomly distributed C and P (and H), with some degree of chemical bonding being present between the C and P. The amorphous nature of these films, plus the lower C—P bond strength (compared to C—C), is consistent with the films becoming softer with increasing P content.

The variation in optical band gap with P content in the film is shown in Fig. 5. The measured values are similar to those obtained in the P-doped films of Ref. [10] of ~1.9–2.0 eV. The deduced increase in band gap from ~2.5 to 3.3 eV with increasing P content could be explained in terms of a decrease in concentration of sp^2 sites within the film [19], consistent with the idea that the films become more amorphous at these higher P contents.

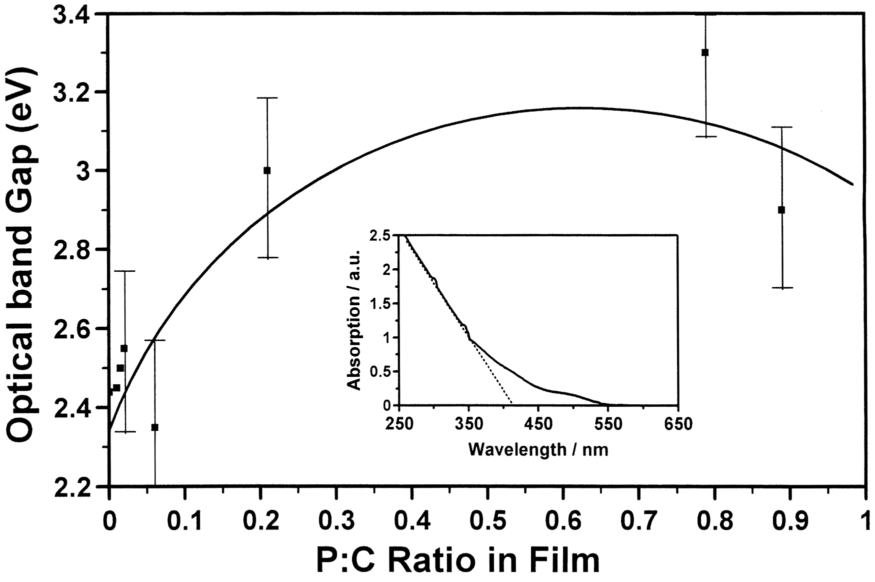

Fig. 5. The variation in optical band gap measured using the Tauc plot [15] from ultraviolet–visible absorption spectra versus P:C ratio in the film. Errors in the band gap value obtained by this method are estimated to be ~ ±0.2 eV, and a smooth curve has been drawn through the points to guide the eye to the general trend. The inset gives an example of a ultraviolet–visible absorption spectrum for the film having a P:C ratio of 0.22 showing the extrapolation of the linear part of the curve to give the Tauc band gap of 415 nm (≡3.0 eV).

Fig. 6 shows the results from field emission experiments, plotted as a function of P content in the films. Ongoing work in our group has shown the threshold voltage to increase roughly linearly with film thickness. Thus, in Fig. 6 the threshold fields have been scaled to remove the effects of variation in film thickness. We define this scaled quantity — the 'threshold field density' (in units of V μm^{-2}) — to be the threshold field divided by film thickness. Fig. 6 shows that this field emission threshold density (as-grown sample) increases steeply with increasing dopant concentration, reaching a maximum value of almost double that of an undoped film at a P:C ratio of 0.001 in the film. With further increases in P content, the threshold density falls rapidly reaching a minimum of ~70% of the value for the undoped film at a P:C ratio of ~0.02. Thereafter, the threshold density gradually increases again as the film becomes more amorphous. Indeed, the threshold density parallels the measured increase in band gap rather closely. After annealing, we found that the films had decreased in thickness by an average of ~10%. Those films with a very low P content have threshold densities much lower (25–50%) than the as-grown films, but films with P:C ratios >0.025 have threshold densities comparable to the as-grown films.

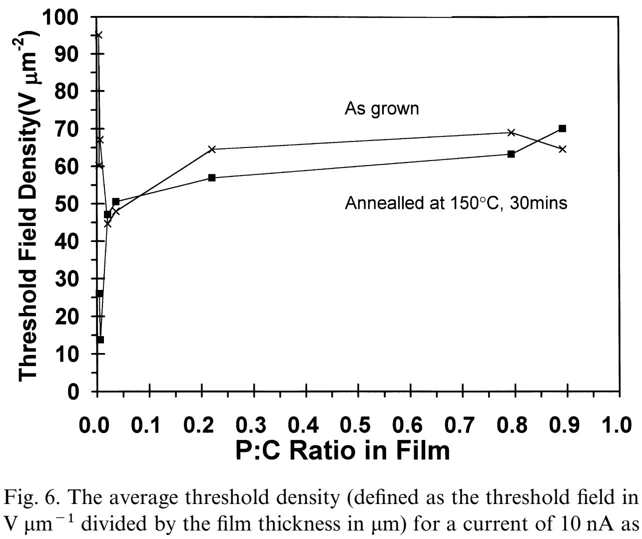

Fig. 6. The average threshold density (defined as the threshold field in V μm^{-1} divided by the film thickness in μm) for a current of 10 nA as a function of the P:C ratio in the films. The two curves are for an as-grown film (×) and a film annealled in vacuum for 30 min at 150°C (■).

4. Conclusions

The P:C films deposited in these experiments appear to fall into three different regimes, corresponding to different P content. The first regime is for films having a P:C ratio of <0.025, which behave like poor quality DLC films. The P does not seem to be incorporated in an electronically active form and in fact degrades the electrical properties, presumably by damaging some of the conducting pathways within the film. Compared to the undoped DLC films, these films have higher field emission threshold densities and an increased optical band gap. However, the films in this regime can be improved substantially by a vacuum annealing process. The second regime is for films having a P:C ratio of 0.025–0.05 for which the field emission threshold density is considerably improved over that for undoped films.

The final regime is for films having a P:C ratio of >0.05 in which P atoms gradually become a larger fraction of the film composition, so destroying the long–medium range structure associated with C—C bonding, and with it the conducting pathways necessary for good electrical properties.

We can conclude from these arguments that the optimum P:C ratio in these films for field emission properties is around 0.02, however even at this value the electrical properties are still only slightly better than those in the undoped films. This could be because much of the P is incorporated in an electrically non-active form. Attempts at ‘activating’ the P by post-deposition annealing showed promise, particularly at low P doping levels, but many more annealing conditions (temperature, background ambient, time) need to be investigated.

One potential problem with these films is their apparent sensitivity to air, with the propensity for the more heavily P-doped samples to oxidise after exposure to air for a few hours or days. This alters the surface characteristics significantly and can affect contact resistance and field emission values. This air sensitivity not only makes it a problem to obtain repeatable and reproducible data from these films, but may also be a limiting factor for their utilisation in practical electronic devices. Clearly, the subject of P-doped DLC films is a very new area of research and much more work needs to be done to fully understand all the complex features of this system.

Acknowledgements

The authors would like to thank J. Hayes and Professor J.W. Steeds of the Bristol University Physics Department for Raman spectroscopy analysis, and J. Eccles of Millbrook Instruments for SIMS analysis. PWM also wishes to thank the Royal Society for funding and the award of a University Research Fellowship.

References

[1] S.R.P. Silva, J. Robertson, W.I. Milne, G.A.J. Amaratunga, Amorphous Carbon State of the Art, World Scientific, Singapore, 1998.

[2] J. Robertson, C.A. Davis, Diamond Relat. Mater. 4 (1995) 441.

[3] G.A.J. Amaratunga, S.R.P. Silva, Appl. Phys. Lett. 68 (1996) 2529.

[4] M.Y. Chen, P.T. Murray, J. Vac. Sci. Technol. A 16 (1998) 2093.

[5] K. Okano, S. Koizumi, S.R.P. Silva, G.A.J. Amaratunga, Nature 381 (1996) 140.

[6] M-T. Kuo, P.W. May, A. Gunn, J.C. Marshall, M.N.R. Ashfold, K.N. Rosser (in press). Int. J. Mod. Phys. B: Condens. Matter Phys.

[7] R.S. Tsang, P.W. May, M.N.R. Ashfold, K.N. Rosser, Diamond Relat. Mater. 7 (1998) 1651.

[8] S. Koizumi, M. Kamo, Y. Sato, S. Mita, A. Sawabe, A. Reznik, C. UzanSaguy, R. Kalish, Diamond Relat. Mater. 7 (1998) 540.

[9] D.I. Jones, A.D. Stewart, Philos. Mag. B 46 (1982) 423.

[10] V.S. Veerasamy, G.A.J. Amaratunga, C.A. Davis, A.E. Timbs, W.I. Milne, D.R. McKenzie, J. Phys.: Condens. Matter 5 (1993) L169.

[11] A. Helmbold, P. Hammer, J.U. Thiele, K. Rohwer, D. Meissner, Philos. Mag. B 72 (1995) 335.

[12] M.M. Golzan, D.R. McKenzie, D.J. Miller, S.J. Collocott, G.A.J. Amaratunga, Diamond Relat. Mater. 4 (1995) 912.

[13] C.A. Davis, Y. Yin, D.R. McKenzie, L.E. Hall, E. Kravtchinskaia, V. Keast, G.A.J. Amaratunga, V.S. Veersamy, J. Non-Cryst. Solids 170 (1994) 46.

[14] L.E. Davis, N.C. MacDonald, P.W. Palmberg, G.E. Riach, R.E. Weber, Handbook of Auger Electron Spectroscopy, Physical Electronic Industries, Minnesota, 1976.

[15] J. Tauc, in: F. Abeles (Ed.), Optical Properties of Solids, North-Holland, Amsterdam, 1972, p. 270.

[16] P.W. May, S. Höhn, M.N.R. Ashfold, W.N. Wang, N.A. Fox, T.J. Davis, J.W. Steeds, J. Appl. Phys. 84 (1998) 1618.

[17] K.M. McNamara, B.E. Williams, K.K. Gleason, B.E. Scruggs, J. Appl. Phys. 76 (1994) 2466.

[18] J. Gerber, M. Weiler, O. Sohr, K. Jung, H. Ehrhardt, Diamond Relat. Mater. 3 (1994) 506.

[19] J. Robertson, M.J. Rutter, Diamond Relat. Mater. 6 (1997) 212.